



Original Articles

Cannabidiol-induced apoptosis is mediated by activation of Noxa in human colorectal cancer cells



Soyeon Jeong^{a,1}, Hye Kyeong Yun^{b,1}, Yoon A Jeong^b, Min Jee Jo^b, Sang Hee Kang^c, Jung Lim Kim^a, Dae Yeong Kim^b, Seong Hye Park^b, Bo Ram Kim^a, Yoo Jin Na^b, Sun Il Lee^c, Han Do Kim^d, Dae Hyun Kim^d, Sang Cheul Oh^{a,b,**}, **Dae-Hee Lee^{a,b,*}**

^a Department of Oncology, Korea University Guro Hospital, Korea University College of Medicine, Seoul, South Korea

^b Graduate School of Medicine, College of Medicine, Korea University, Seoul, 08308, Republic of Korea

^c Department of Surgery, Korea University Guro Hospital, Korea University College of Medicine, Seoul, Republic of Korea

^d Kaiyon Bio Tech Co., Ltd, 226 Gamasan-Ro, Guro-gu, Seoul, 08308, Republic of Korea

ARTICLE INFO

Keywords:

Marijuana extract
Bcl-2 protein family
ROS
Apoptotic cell death
Colon cancer

ABSTRACT

Cannabidiol (CBD), one of the compounds present in the marijuana plant, has anti-tumor properties, but its mechanism is not well known. This study aimed to evaluate the apoptotic action of CBD in colorectal cancer (CRC) cells, and focused on its effects on the novel pro-apoptotic Noxa-reactive oxygen species (ROS) signaling pathway. CBD experiments were performed using the CRC cell lines HCT116 and DLD-1. CBD induced apoptosis by regulating many pro- and anti-apoptotic proteins, of which Noxa showed significantly higher expression. To understand the relationship between Noxa and CBD-induced apoptosis, Noxa levels were downregulated using siRNA, and the expression of apoptosis markers decreased. After ROS production was blocked, the level of Noxa also decreased, suggesting that ROS is involved in the regulation of Noxa, which along with ROS is a well-known pro-apoptotic signaling agents. As a result, CBD induced apoptosis in a Noxa-and-ROS-dependent manner. Taken together, the results obtained in this study re-demonstrated the effects of CBD treatment *in vivo*, thus confirming its role as a novel, reliable anticancer drug.

1. Introduction

Colorectal cancer (CRC) is the fourth leading cause of cancer-related deaths worldwide [26]. Although the development in chemotherapy for CRC has increased overall survival, side effects such as cytotoxicity and resistance continue to limit its utilization. Therefore, there is an urgent need to develop more effective agents for CRC patients.

Noxa is a pro-apoptotic member belonging to the Bcl-2 protein family that is unique in that it contains only Bcl-2 homology 3 domain [16]. During apoptosis, activated Noxa is translocated to the mitochondria, inducing cytochrome c release and subsequent caspase-9 activation [22]. Noxa induces Bax-mediated mitochondrial dysfunction via indirect inhibition of the anti-apoptotic Bcl-2 protein family members [23]. Because Noxa plays a key role in apoptotic cell death, it serves as excellent intracellular target that is an effective therapeutic

target for cancer [4,11]. Noxa is activated by various factors such as ultraviolet radiation, etoposide, hypoxia, mitogenic stimulation, and reactive oxygen species (ROS).

ROS, including O₂⁻ (superoxide radical), ●OH (hydroxyl radical), and H₂O₂ (hydrogen peroxide), play a major role in numerous cellular events [8]. In mammalian cells, the mitochondrial electron transport chain is the primary sites of ROS generation [12]. Excessive ROS can induce mitochondrial dysfunction by decreasing the mitochondrial membrane potential and causing electron leakage, leading to apoptosis [3,6,12].

Cannabidiol (CBD) is one of the best known cannabinoid family, which includes the members of the *Cannabis sativa* family [25]. Cannabinoids interact with specific Gαi protein-coupled receptors, CB₁ (Central receptor) and CB₂ (Peripheral receptor) [31]. However, CBD does not bind well to CB₁ and CB₂ receptors, and the mechanism

* Corresponding author. Division of Oncology/Hematology, Department of Internal Medicine, College of Medicine, Korea University Medical Center, Korea University, Seoul, 08308, Republic of Korea.

** Corresponding author. Division of Oncology/Hematology, Department of Internal Medicine, Korea University Guro Hospital, 148, Gurodong-gil, Guro-gu, Seoul, 08308, South Korea.

E-mail addresses: sachoh@korea.ac.kr (S.C. Oh), neogene@korea.ac.kr (D.-H. Lee).

¹ These authors contribute this work equally.

underlying its actions is not fully known [32]. CBD is a non-psychoactive cannabinoids that exerts anticancer activity in different types of tumors [2,5,33]. It is already a part of many clinical trials for the treatment of glioma [27]. CBD induces autophagy as well as apoptosis in human breast and prostate cancer cells by activating extracellular signal-regulated kinases and inhibiting AKT/mammalian target of rapamycin signaling [25,27]. However, little is known about the mechanisms underlying CBD-induced apoptosis in CRC.

In this study, we investigated the apoptotic cell death induced by CBD in CRC cells, and identified the relationship between Noxa activation and CBD-induced cytotoxicity. We suggest, for the first time, that CBD can cause Noxa-induced cell death. Our results show that CBD induced apoptotic cell death via ROS/endoplasmic reticulum (ER) stress-regulated Noxa activation, suggesting that CBD has important implications for the potential treatment of human CRC.

2. Materials and methods

2.1. Reagents and antibodies

CBD (Sigma, St. Louis, MO, USA) dissolved in absolute Ethanol (EtOH) was stored at 4 °C until use. The antibodies used and their sources were as follows: Cleaved Poly (ADP-ribose) polymerase (PARP), Caspase-3, Caspase-9, Cleaved Caspase-8, Noxa, phospho-PKR-like ER-resistant kinase (PERK), p-PERK, phospho-inositol requiring enzyme-1 α (IRE1 α), p-IRE1 α , Bip, Activating transcription factor 6 (ATF6), Glucose Regulated Protein 94 (GRP94) were purchased from Cell Signaling (Beverly, MA, USA). Anti- β -Actin was purchased from Sigma (St. Louis, MO, USA). The secondary antibodies, anti-mouse-IgG-HRP was purchased from Santa Cruz Biotechnology and anti-rabbit-IgG-HRP was purchased from Cell Signaling Technology.

2.2. Cell culture

Human CRC HCT116 and DLD-1 cells, and human colorectal normal CCD-18Co cells were obtained from the American Type Culture Collection (ATCC, Manassas, VA, USA) and HCT116 Luc⁺ cells were obtained from JCRB Cell Bank. HCT116 and HCT116 Luc⁺ cells were cultured in McCoy's 5A medium. DLD-1 cells were cultured in RPMI 1640 medium, and CCD-18Co cells were cultured in Eagle Minimum Essential Medium (EMEM, ATCC). All media contained 10% fetal bovine serum (HyClone, Logan, UT, USA) and 1% antibiotic-antimycotic solution (100X; GenDEPOT, TX, USA). All cell lines were incubated in a 5% CO₂ incubator at 37 °C.

2.3. Microarray assay

RNA was isolated from the cultured cells using TRIzol and RNA purity and integrity were confirmed by ND-1000 Spectrophotometer (NanoDrop, DE, USA) and Agilent 2100 Bioanalyzer (Agilent Technologies, CA, USA). Next, the Affymetrix Whole transcript Expression array method was proceeded according to the manufacturer's manual (GeneChip Whole Transcript PLUS reagent Kit). The cDNA was synthesized by using the GeneChip Whole Transcript Amplification kit which described by the manufacturer. The sense strand of the cDNA was then fragmented. It was biotin-labeled with terminal deoxynucleotidyl transferase by using the GeneChip WT Terminal labeling kit. Approximately 5.5 μ g of targeted DNA, which was labeled, was hybridized in the Affymetrix GeneChip 2.0 ST Array at 45 °C for 16 h. Hybridized arrays were washed and scanned on a GCS3000 Scanner (Affymetrix) after staining at a GeneChip Fluidics Station 450. Signal values were computed by using the Affymetrix® GeneChip™ Command Console software.

2.4. WST-1 assay

Cell viability was measured using the Cell Viability Assay Kit (EZ-Cytox, DOGEN, Daejeon, Republic of Korea). HCT116 cells (1×10^4 cells per well) and DLD-1 cells (8×10^3 cells per well) were seeded in 96-well plates, and incubated in 5% CO₂ incubator at 37 °C for 24 h. Then, the cells were treated with CBD in serum-free medium for 24 h in under identical condition. The cells were then treated with EZ-Cytox for additional 2 h, and then subjected to detection.

2.5. Colony formation assay

Colony formation assay was used to study the proliferation of cells. The cells were seeded in a 60 π (60 \times 15 mm) cell culture dish. After 24 h of incubation, the cells were subjected to CBD treatment for another 24 h. Trypsin-ethylenediaminetetraacetic acid (Trypsin-EDTA, GenDEPOT) was used to detach the cells, and the cells were seeded in 6-well plates. After 2 weeks, the cells were stained with the colony formation assay solution.

2.6. Immunoblotting analysis

To prepare cell lysates, lysis buffer (containing protease inhibitor, phosphatase inhibitor, and RIPA buffer) was added, and the cells were lysed by sonication. The suspension was then centrifuged. The protein content of the supernatant was quantified using the bicinchoninic acid assay kit (Pierce™ BCA Protein Assay Kit, Thermo Fisher Scientific, MA, USA) and 5X sample buffer. Proteins were separated using 8–12% sodium dodecyl sulfate-polyacrylamide gels, and then transferred to a nitrocellulose blotting membrane. About 10% bovine serum albumin (BSA) was used as a blocking buffer for 1 h at room temperature (RT). The membrane was then probed with primary antibodies, which were diluted in a primary antibody dilution solution (0.5% BSA with 0.1% sodium azide; 1:1000), overnight at 4 °C. The membranes were then washed with 1X Tris-buffered saline containing Tween 20 (TBST). Membranes were then probed with the specific secondary antibodies for 2 h at 4 °C, and then detected with the electrochemiluminescence solution (EZ-Western Lumi Pico; DOGEN).

2.7. Flow cytometry analysis

Translocation was detected based on the binding of allophycocyanin-conjugated Annexin V. The cells were harvested using Trypsin-EDTA, without causing any harm to the cells. The harvested cells were then mixed with a mixture of Annexin V, phosphatidylinositol reagent, and 1X binding buffer from Annexin V-FITC Apoptosis Detection Kit (BioBud, Seoul, Republic of Korea). After 30 min at RT without light, the cells were analyzed using flow cytometry.

2.8. Terminal deoxynucleotidyl transferase dUTP nick end labeling (TUNEL) assay

TUNEL assay was used to detect apoptosis and was performed using In Situ Cell Death Detection Kit (Roche Diagnostics GmbH, Mannheim, Germany). The cells were first fixed with 3.7% formaldehyde and then permeabilized with 0.5% Triton X-100 for 15 min at RT. Nuclei were stained with 4',6-diamidino-2-phenylindole (DAPI, Invitrogen, CA, USA) for 20 min at 37 °C in 5% CO₂ incubator. After washing the cells three times with TBST, the mixture from the assay kit was used to stain dead cells. The cells were then incubated for 1 h at 37 °C in a 5% CO₂ incubator. These cells were observed by confocal microscopy.

2.9. RNA interference assay

HCT116 and DLD-1 cells were transfected with Noxa siRNA and CHOP siRNA purchased from Santa Cruz Biotechnology (Santa Cruz).

Prior to siRNA treatment, the opti-minimum essential medium (Opti-MEM; Gibco, Life Technologies, LA, USA) was added to the dish and incubated at 37 °C for 30 min to warm the cells. Then, the mixture containing siRNA, Opti-MEM, and Lipofectamine RNAiMAX (Invitrogen) was incubated for 30 min at RT. The mixture was then added to the warmed cells and incubated for 18 h at 37 °C in a 5% CO₂ incubator. The cells were then treated with CBD for subsequent analysis.

2.10. RNA extraction for reverse-transcriptase polymerase chain reaction (RT-PCR) and quantitative real time PCR (qRT-PCR)

TRIzol reagent (TRI reagent, Molecular Research Center, OH, USA) was used for extraction of RNA, according to the manufacturer's instructions. After lysing the cells, cold chloroform was added and the solution was kept on ice for 30 min and centrifuged for 10 min at 12,000 rpm (14,240 × g) at 4 °C. Then, the supernatant was transferred to another tube. Cold isopropanol was added to precipitate the RNA. After gentle mixing, the sample was incubated for 20 min on ice and centrifuged for 10 min at 12,000 rpm (14,240 × g). The RNA pellet was then washed with 75% EtOH (diluted with diethyl pyrocarbonate, DEPC). After the pellet was air-dried, it was dissolved in DEPC water and concentrated. RT-PCR assay was performed using the RT-PCR kit (Life Technologies). qRT-PCR was used to determine mRNA levels of Noxa, and GAPDH was used as control. Taqman Probes were purchased from Thermo Fisher Scientific for Noxa and GAPDH.

2.11. Immunocytochemistry assay

HCT116 and DLD-1 cells were seeded on a glass coverslip. The treated cells were fixed with 3.7% formaldehyde for 15 min at RT, and then, 0.5% Triton X-100 was used for permeabilization under same conditions. The cells were blocked with 3% BSA for 1 h, and then incubated overnight with primary antibodies, both at 4 °C. DAPI was used to stain the nuclei of cells, followed by the specific secondary antibodies (17 min at 4 °C).

2.12. ROS detection assay

2',7'-Dichlorodihydrofluorescein Diacetate (DCF-DA, Invitrogen) reagent was used to detect total cell ROS, while mitochondrial superoxide indicator (MitoSOX, Invitrogen) reagent was used to detect mitochondrial ROS. Tetramethylrhodamine, ethyl ester, perchlorate (TMRE, Thermo Fisher Scientific) was used to measure the mitochondrial transmembrane potential (MMP). For fluorescence staining, the cells, seeded on a coverslip, were fixed and permeabilized with 3.7% formaldehyde and 0.5% Triton X-100 for 15 min at RT. The nuclei were stained with DAPI, followed by treatment with the ROS detection reagents, namely, DCF-DA and MitoSOX, for 10 min at 37 °C. The treated cells were then observed by confocal microscopy. For flow cytometry analysis, the seeded cells were treated with MitoSOX and TMRE, 30 min, 1 h and 6 h after CBD treatment and incubated for 30 min at 37 °C.

2.13. Chromatin immunoprecipitation (ChIP) assay

For the ChIP assay, 1% formaldehyde was directly added to HCT116 and DLD-1 cells (1.5 × 10⁶ cells per dish) to facilitate the cross-linking of proteins to DNA. After the incubation for 15 min at 37 °C, the cells were harvested with a cell scraper and then centrifuged. Pellets were resuspended in SDS lysis buffer containing phenylmethane sulfonyl fluoride (PMSF) and a protease inhibitor and then incubated on ice for 10 min. Cell lysate was sonicated in various conditions to obtain 200 and 1000 base-pair DNA fragments. Lysates were immunoprecipitated with anti-CHOP, anti-ATF3 and anti-ATF4 overnight at 4 °C. The protein-DNA complex was incubated with protein A/salmon sperm DNA

for 1 h at 4 °C, washed, eluted with TE and 1% SDS, and the protein/DNA was reverse cross-linked with protease K, EDTA, and Tris-HCl. Phenol:Chloroform:Isoamyl alcohol (25:24:1) extraction was used to purify DNA followed by precipitation with ethanol. The isolated DNA was amplified by PCR using the following specific primer: P1 forward, 5' GCT ACT CAA AGT TGT CCA CAG AGC 3'; reverse, 5' GGT GGA GAG ACC AGT AAC TCA GAA 3' and P2 forward, 5' AGT AAG GCC AGA CAG CAA CAT C 3'; reverse, 5' GAA TCC TCC AGA ACT CTA GCC AAG 3', P3 forward, 5' GGG CTT GTT TAC CCA AGT CTC TA 3'; reverse, 5' GCC CCG AAA TTA CTT CCT TAC A 3' and P4 forward, 5' TCC TGA TGT CAG CTA ATG TCT CTG 3'; reverse, 5' CCT CAC GGA CAT GAC ATT TCT A 3'.

2.14. Patient-derived colorectal cancer (PDC) cells

These cells were derived from tissue samples donated by colorectal cancer patients. The Institutional Review Board of Guro Hospital (KUGH16275) provided an approval to the Korea University Guro Hospital Tissue Bank to obtain such tissue samples. The tissue samples were first chopped with a disposable knife and then stored in the tissue grinder tube, filled with DMEM. Collagenase (final concentration to 0.5%) and accutase (final concentration to 10%) were then added to the medium, which contained the tissue and the tissue was then ground. After incubation at 37 °C for 30 min, the ground tissue was filtered with a strainer and then centrifuged for 2 min at 2000 rpm. Pellets were then suspended with the medium and then seeded to the dish.

2.15. Caspase 3/7 detection analysis

IncuCyte[®] Caspase-3/7 Reagent (Essen BioScience, MI, USA) was used to measure caspase 3/7 activities. When the PDC cells were seeded into the three-dimensional 96-well plate, the medium that contained the caspase 3/7 reagent, was then added to the cells. After 30 min of incubation, images of the cells were captured using the IncuCyte[®] system followed by further analysis.

2.16. Animal experiments

Animal experiments were performed in accordance with the guidelines approved by the Korea University Institutional Animal Care and Use Committee (IACUC). Four-week-old female BALB/c nude mice were purchased from Orient Bio (Seong-Nam, Republic of Korea), and grown in a specific pathogen-free environment. HCT116 Luc⁺ cells (1 × 10⁷ cells in 100 μL of PBS) were injected and housed for 1 week. CBD was intraperitoneally injected for every 3 days. The tumor size was also calculated at the same time. The tumor size was calculated using the formula: length × width; the volume was calculated as 0.5 × length × (width)². Five mice were examined in each treatment group.

2.17. Immunohistochemistry assay

The harvested tissue, maintained in 4% paraformaldehyde, was processed for embedding. After the tissue was inserted into the cassettes, it was drained (70% EtOH, for 1 h; 95% EtOH, twice for 30 min; 100% EtOH, three times for 30 min; and Xylene, three times for 30 min). Then, the cassettes were maintained overnight in molten paraffin. The paraffin-embedded and sections were used for the immunohistochemical assay. The tissues were then hydrated (Xylene, three times for 10 min; 100% EtOH, twice for 10 min; 95% EtOH, twice for 10 min; 70% EtOH, for 5 min, and distilled water (DW), three times for 10 min). The tissue was then treated with 30% H₂O₂ (diluted with DW) for 15 min, followed by washing with DW three times for 10 min. The retrieval solution (Dako REAL Target Retrieval Solution (10X); Dako, Glostrup, Denmark), prepared using a microwave, was used to retrieve the tissue. After washing the tissue with DW three times for

10 min, the Dako pen was used to draw the border of the tissue. Then, the blocking solution (Universal Blocking Reagent; Biogenex, CA, USA) was added to the boundary, and the tissue was blocked for 15 min at RT. The tissue was incubated with the primary antibody (diluted 1:200), overnight at 4 °C. To wash the primary antibody, PBS with Tween 20 (PBST) was used three times for 10 min, and the bubbles were removed with DW. Then, the secondary antibody was incubated with the tissue for 1 h at RT, and then washed with PBST three times for 10 min. After removing the bubbles with DW, the mounting solution containing DAPI was used for mounting. The tissue was observed by confocal microscopy.

2.18. Statistical analysis

Each experiment was conducted independently and repeated a minimum of three times. Statistical analyses were conducted using GraphPad InStat 6 Software. These included the unpaired Student's *t*-test. In all analyses, the level of statistical significance was more than the 95% confidence level ($P < 0.05$). $P < 0.05$ was considered statistically significant.

3. Results

3.1. CBD inhibits cell viability and induces apoptosis in human CRC cells

To investigate the ability of CBD to induce apoptotic cell death in CRC cells, various human CRC cells were cultured with different concentrations (0–8 μM) of CBD for 24 h, and the cell viability was measured by WST-1 assay. As shown in Fig. 1A, CBD decreased the viability of CRC cells in a dose-dependent manner, but not of normal primary colorectal CCD-18Co cells and normal primary lung Beas2B cells (Fig. 1A). To examine the long-term effect on clonogenic survival treated cells, colony formation assay was performed. This ability was reduced by CBD treatment (Fig. 1B).

To determine whether the decreased viability of CBD-treated cells could be attributed to apoptosis, HCT116 and DLD-1 cells were treated with CBD and tested for apoptotic changes. CBD caused a dose- and time-dependent increase in the expression of cleaved PARP, caspase-3, -8 and -9 (Fig. 1C and D), which are widely used apoptotic marker [9]. Furthermore, CBD significantly elevated the number of Annexin V/PI double-stained cells (Fig. 1E) and TUNEL-positive cells (Fig. 1F), indicating that CBD induces apoptosis.

3.2. Noxa activation is responsible for CBD-induced apoptosis

Since Noxa plays important roles in the regulation of apoptosis [17], we confirmed the levels of Noxa mRNA and protein. Immunoblotting analysis showed that CBD increased the mRNA and protein levels of Noxa in a time-dependent manner (Fig. 2A, B and 2C). In addition, the fluorescence intensity of Noxa was significantly higher in CBD-treated cells, compared to the control cells (Fig. 2D).

To unveil the role of Noxa activation in CBD-induced apoptosis, CRC cells were transfected with Noxa-specific siRNA. Compared to the cells treated with control siRNA, Noxa knockdown attenuated CBD-induced apoptotic cell death in both cell lines, as shown by the numbers of Annexin V/PI double-stained cells as well as levels of PARP, caspase-3, -8 and -9 cleavage (Fig. 2E, F, and 2G).

Since Noxa is regulated by p53 [24], we examined whether CBD-induced Noxa activation is associated with p53. Microarray and western blot results showed that p53 was increased by CBD. However, when p53 was knocked out, p53 was not changed, but Noxa and apoptosis were increased (Suppl. Fig. 1A and 1B). Taken together, these findings demonstrated that Noxa plays an important role in apoptotic cell death by CBD independently of p53 in CRC cells.

3.3. CBD induces ROS generation and endoplasmic reticulum (ER) stress

To elucidate the mechanisms underlying CBD-induced apoptosis, microarray analysis was performed. Gene set enrichment analysis showed that ROS and unfolded protein response (UPR) were increased by CBD treatment (Fig. 3A). Therefore, we examined the potential involvement of ROS production in CBD-induced apoptosis. The effect of CBD on the generation of superoxide was investigated by monitoring the intensity of DCF-DA. CBD treatment enhanced intracellular superoxide production, and treatment with NAC, an antioxidant, effectively blocked the levels of intracellular superoxide (Fig. 3B and Suppl. Fig. 2A). Because ROS is mainly produced in the mitochondria [8], we measured mitochondrial ROS production to determine whether the CBD-induced ROS generation was derived in the mitochondria. As shown in Fig. 3C, Suppl. Fig. 2B and 2C, CBD increased mitochondrial superoxide levels from an early time and NAC inhibited this effect of CBD. CBD also induced mitochondrial dysfunction by TMRE fluorescence, an indicator of MMP (Suppl. Fig. 2D). Moreover, antioxidant enzymes including SODs and Catalase were decreased by CBD treatment (Fig. 3D), implying that CBD causes mitochondrial dysfunction and excessive ROS generation especially mitochondrial superoxide.

ROS and ER stress are closely related [13]. Previous studies showed that ROS induces ER stress in CRC cells [1,34]. DLD-1 and HCT116 cells were treated with 6 μM CBD, and the levels of ER stress-related proteins were examined by western blot. CBD dramatically elevated ER transmembrane receptors (IRE1α and PERK), ER chaperone protein (Bip, GRP94), and transcription factor CHOP in a dose- and time-dependent manner (Fig. 3E and F). Together, CBD triggers mitochondrial dysfunction-induced ROS overproduction and excessive ER stress through IRE1α and PERK.

3.4. CBD-induced noxa regulation leads to apoptosis by causing excessive ROS and ER stress

To further explore the role of ROS generation in CBD-induced CRC cell death further, NAC-mediated blockade of ROS was performed. The results showed that the NAC suppressed CBD-induced apoptosis as revealed by the level of cleaved PARP (Fig. 4A) and the number of Annexin V/PI double-stained cells (Fig. 4B), suggesting that CBD triggers ROS overproduction and subsequent apoptosis in human CRC cells. Because Noxa causes mitochondrial dysfunction, which is mainly induced by ROS [22,37], we investigated the possible link between ROS overproduction and Noxa activation in CBD-treated CRC cells. We found that CBD-induced increase in Noxa levels was remarkably attenuated by NAC pre-treatment in both CRC cell lines (Fig. 4A). Together, these findings indicated that ROS overproduction is linked to the Noxa activation, and that CBD-induced apoptotic cell death is responsible for the ROS-mediated Noxa activation.

To confirm that the relationship between ER stress and CBD-induced apoptosis, CRC cells were first transfected with CHOP siRNA. Then, the number of Annexin V/PI double-stained cells and the levels of Cleaved PARP were measured by western blotting and flow cytometry, respectively. CHOP knockdown significantly reversed the increases in both the Cleaved PARP level and Annexin V/PI double-stained cell count (Fig. 4D). Furthermore, CBD activated the Noxa protein and increased the extent of staining levels of Noxa, which could be further blocked by CHOP siRNA (Fig. 4C and F). ChIP assay was performed to confirm that CHOP directly regulates Noxa. As shown in Suppl. Fig. 3A and 3B, CHOP did not bind to the Noxa promoter. Since ATF3 and ATF4 bind to Noxa and CHOP promoter to regulate the apoptosis [15], we examined whether CBD affects the activity of binding to the Noxa and CHOP promoter regions. As shown in Suppl. Fig. 3C and 3D, CBD increased the binding of ATF3 and ATF4 to the promoters of Noxa and CHOP. These data together imply that excessive ER stress contributes to the CBD-dependent Noxa activation and apoptotic cell death by ATF3 and ATF4.

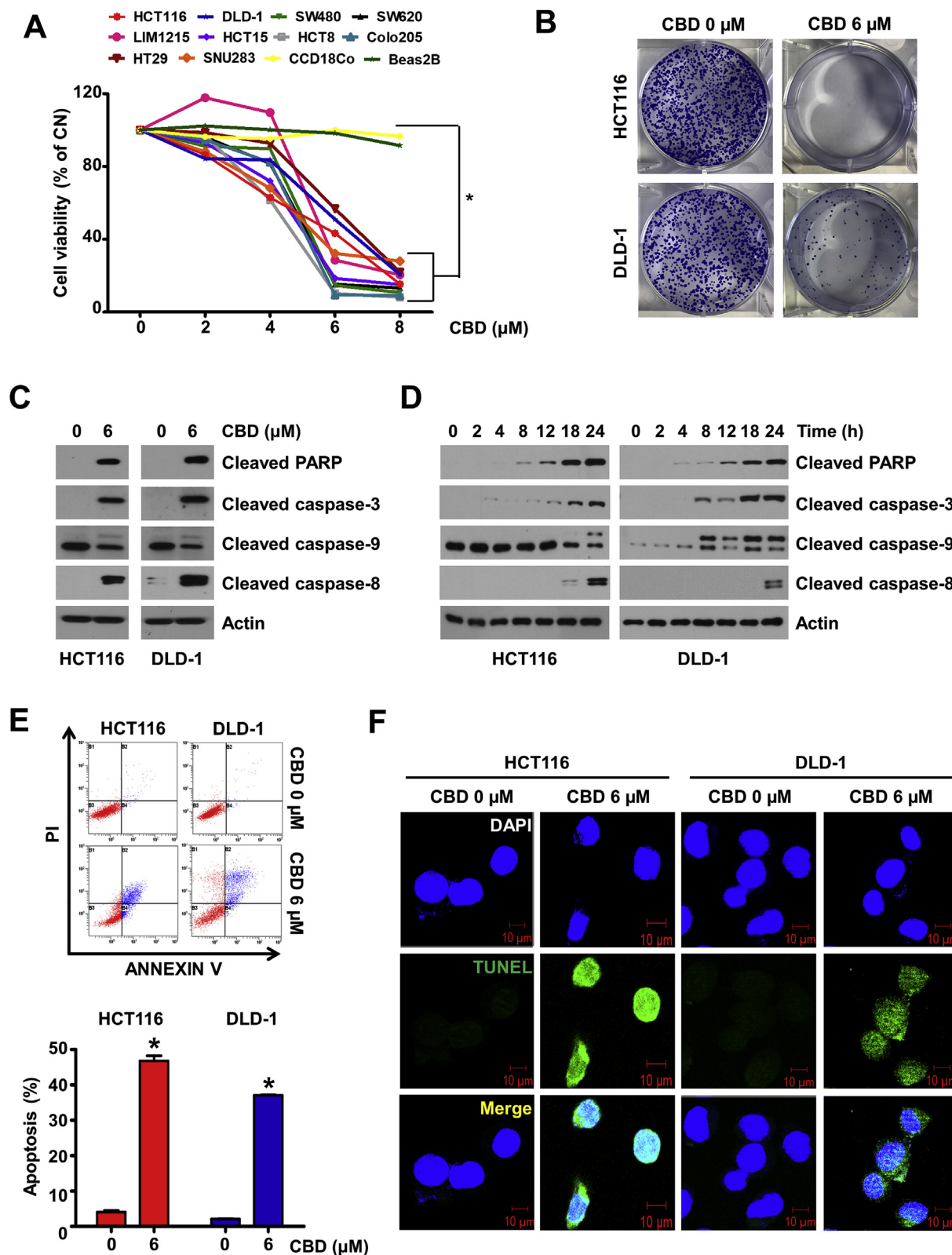


Fig. 1. CBD reduces viability and induces apoptotic cell death of human CRC cells. (A) Normal primary cell lines (CCD-18Co and Beas2B) and various CRC cells were treated with 0, 2, 4, 6, and 8 μM of the CBD for 24 h. The cell viability was detected by WST-1 assay. (B) HCT116 (upper) and DLD-1 (lower) cells were treated with 0 or 6 μM of CBD. After 2 weeks, the cells were stained with crystal violet, and the colonies were photographed using a digital camera. (C–D) The cells were incubated with CBD at the doses (C) and defined time periods (D). The levels of Cleaved PARP, caspase-3, -8, and -9 were analyzed by Western blotting. (E) Cells stained with Annexin V and PI were studied using flow cytometry to detect the apoptosis induced by exposure to 6 μM CBD in CRC cell lines. Values are shown as mean ± standard error of mean (SEM) (n = 5). *, P < 0.05. (F) Cell apoptosis was detected with TUNEL assay, and DAPI was used as a co-stained to dye the nuclei of the HCT116 (left) and DLD-1 (right) cells. After treatment of CBD (6 μM), damaged DNA was visualized in bright green (TUNEL-positive cells), indicating apoptosis (Scale Bar, 10 μm). (For interpretation of the references to color in this figure legend, the reader is referred to the Web version of this article.)

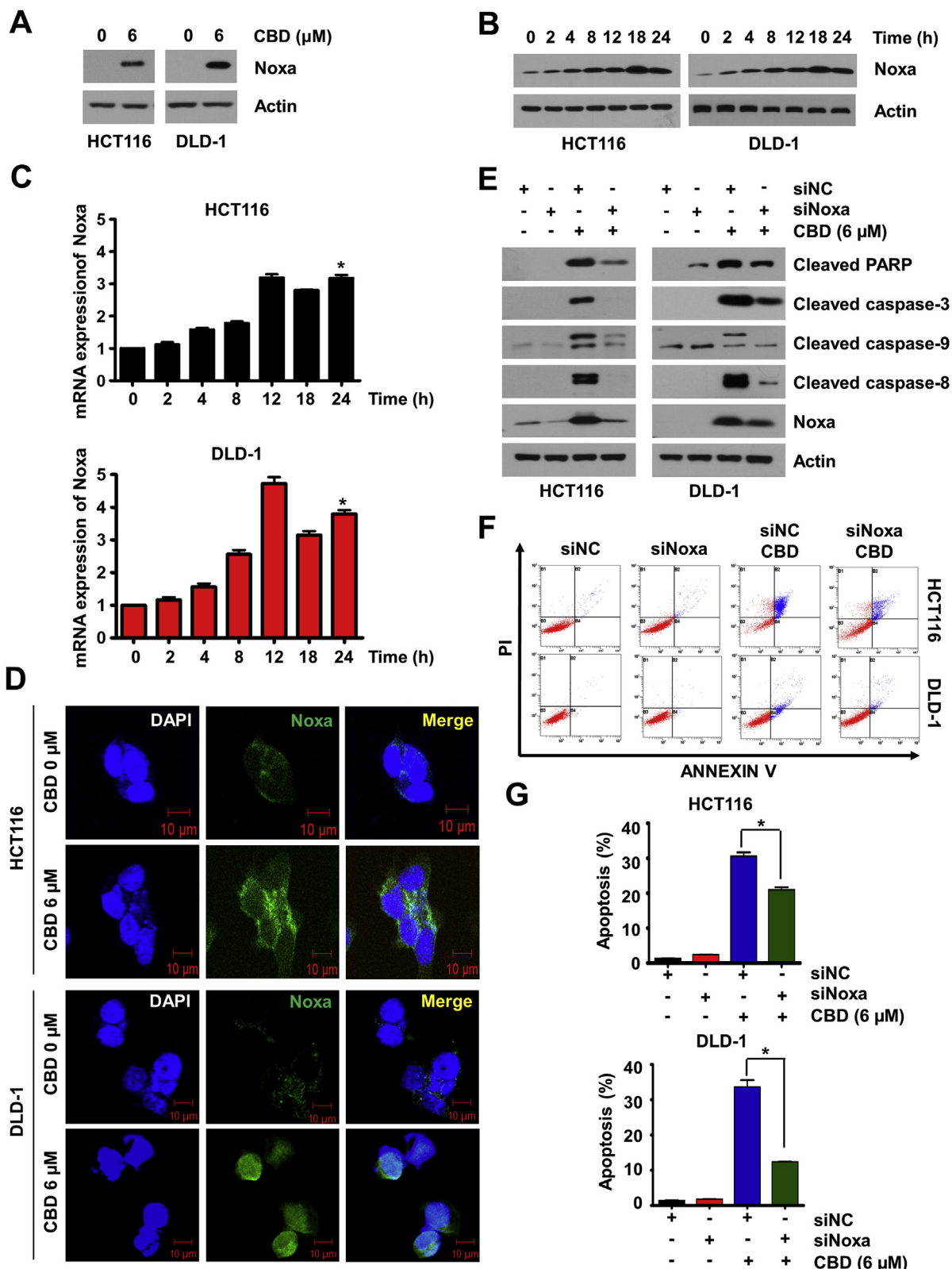


Fig. 2. CBD induces apoptosis by regulating *Noxa*. (A–B) The increase in *Noxa* protein level was confirmed at different doses of CBD (A) and different time periods (B). (C) Treatment with 6 μM CBD resulted in an increase in *Noxa* expression in different time periods. *, $P < 0.05$. (D) Under identical conditions, *Noxa* expression (light green) after treatment with 6 μM CBD was evaluated by confocal microscopy (Scale Bar, 10 μm). (E–G) The cells were transfected with control siRNA or siNoxa and then treated with CBD (6 μM). *Noxa* protein and the apoptosis marker, Cleaved PARP, caspase-3, -8, and -9 were analyzed by western blotting (E), and the rate of apoptosis was observed by flow cytometry (F–G). *, $P < 0.05$. (For interpretation of the references to color in this figure legend, the reader is referred to the Web version of this article.)

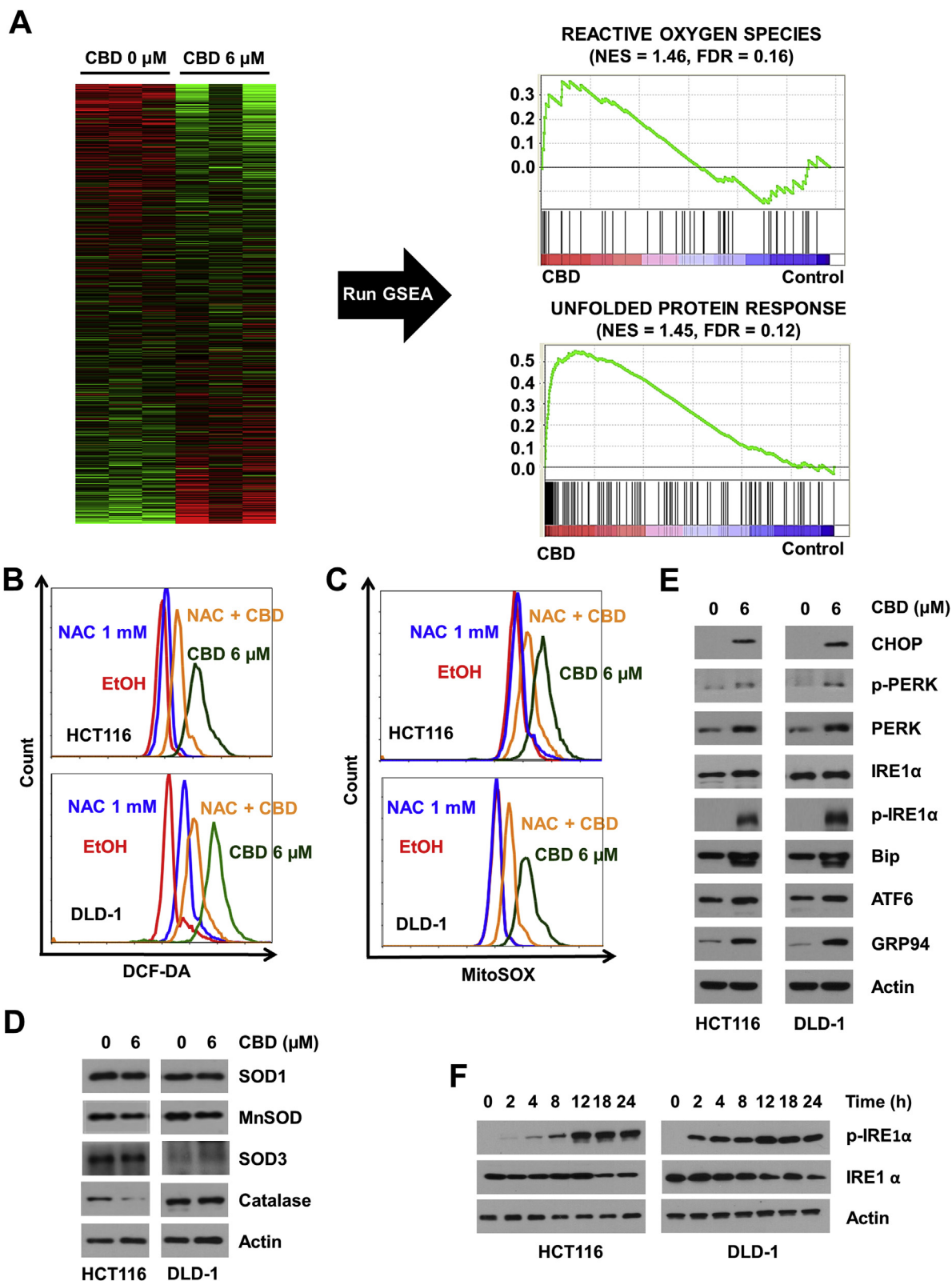


Fig. 3. CBD induces ROS and ER stress. (A) The upregulation of ROS and Unfolded proteins were measured by microarray data. (B–C) HCT116 (upper) and DLD-1 (lower) cells were stained with (B) DCF-DA and (C) MitoSOX after with or without NAC (1 mM), ROS scavenger, and CBD (6 μM) to trace the progress of ROS production, by flow cytometry. (D–E) After treatment of 6 μM CBD, the anti-oxidant proteins (D) and ER stress-related proteins (E) were also confirmed with the western blotting. (F) One of the ER stress markers, p-IRE1α protein was increased in time periods when analyzed with western blotting.

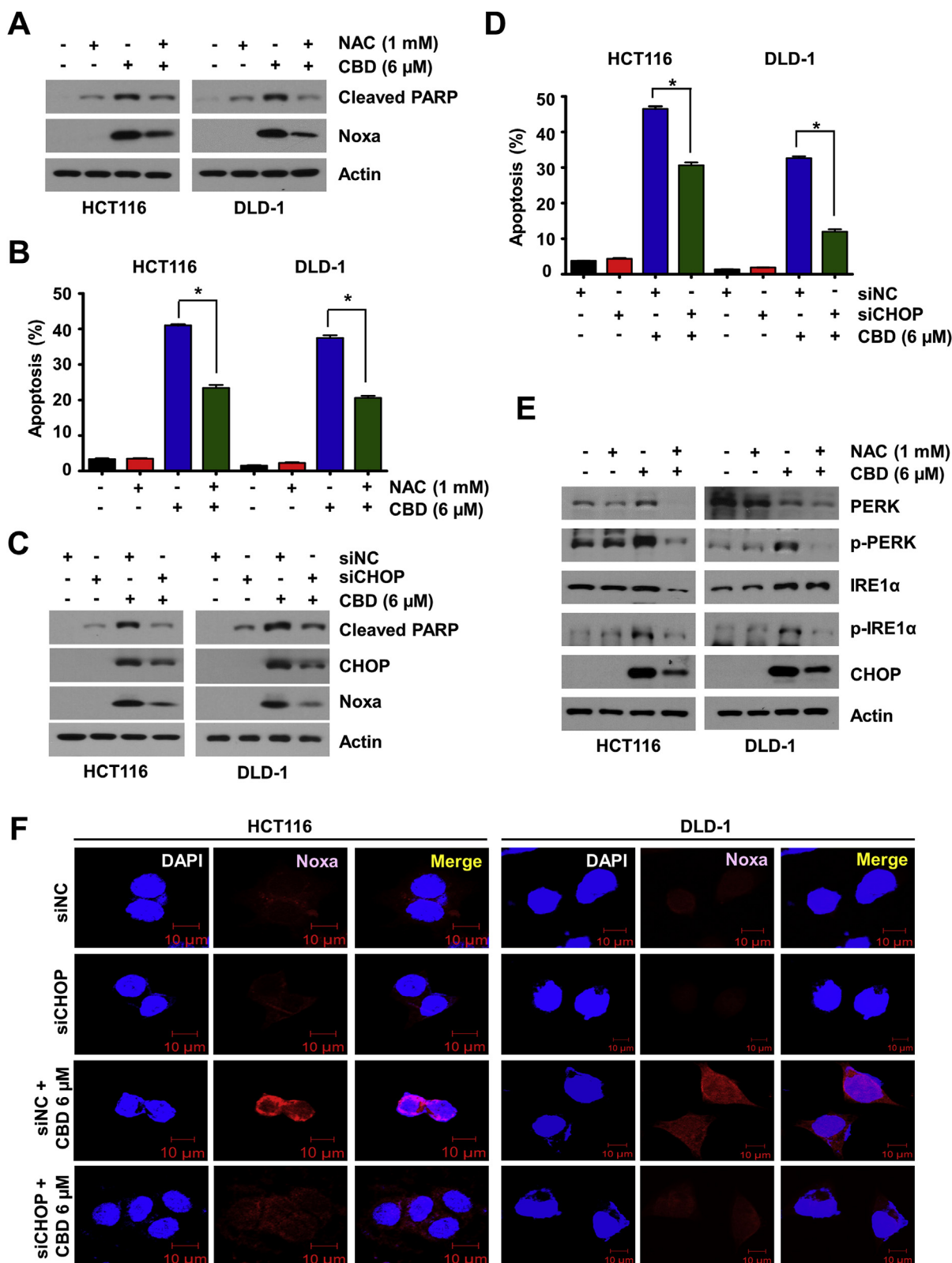


Fig. 4. ROS and ER stress induce apoptosis by regulating the Noxa protein. The cells were treated with NAC (1 mM) or left untreated, and then treated with or without the CBD (6 μM). (A) Cleaved PARP, an apoptosis marker, and Noxa protein were both detected by western blotting. (B) Apoptosis was also confirmed with the flow cytometry in the same condition. The cells treated with both CBD and NAC were less sensitive to apoptosis, compared to those treated with CBD but not NAC. (C–D) HCT116 and DLD-1 cells were transfected with control siRNA or siCHOP, and then treated with CBD (6 μM). The cleaved PARP, CHOP, and Noxa protein were confirmed with western blotting (C) and the apoptosis was detected with flow cytometry (D). *, $P < 0.05$. (E) ER stress sensors, p-PERK, p-IRE1α, and CHOP were confirmed with western blotting after treated with or without NAC (1 mM), and treated with or without CBD (6 μM). (F) Noxa expression after the transfection of control siRNA or siCHOP along with CBD treatment can be detected by confocal microscopy (Scale bar, 10 μm).

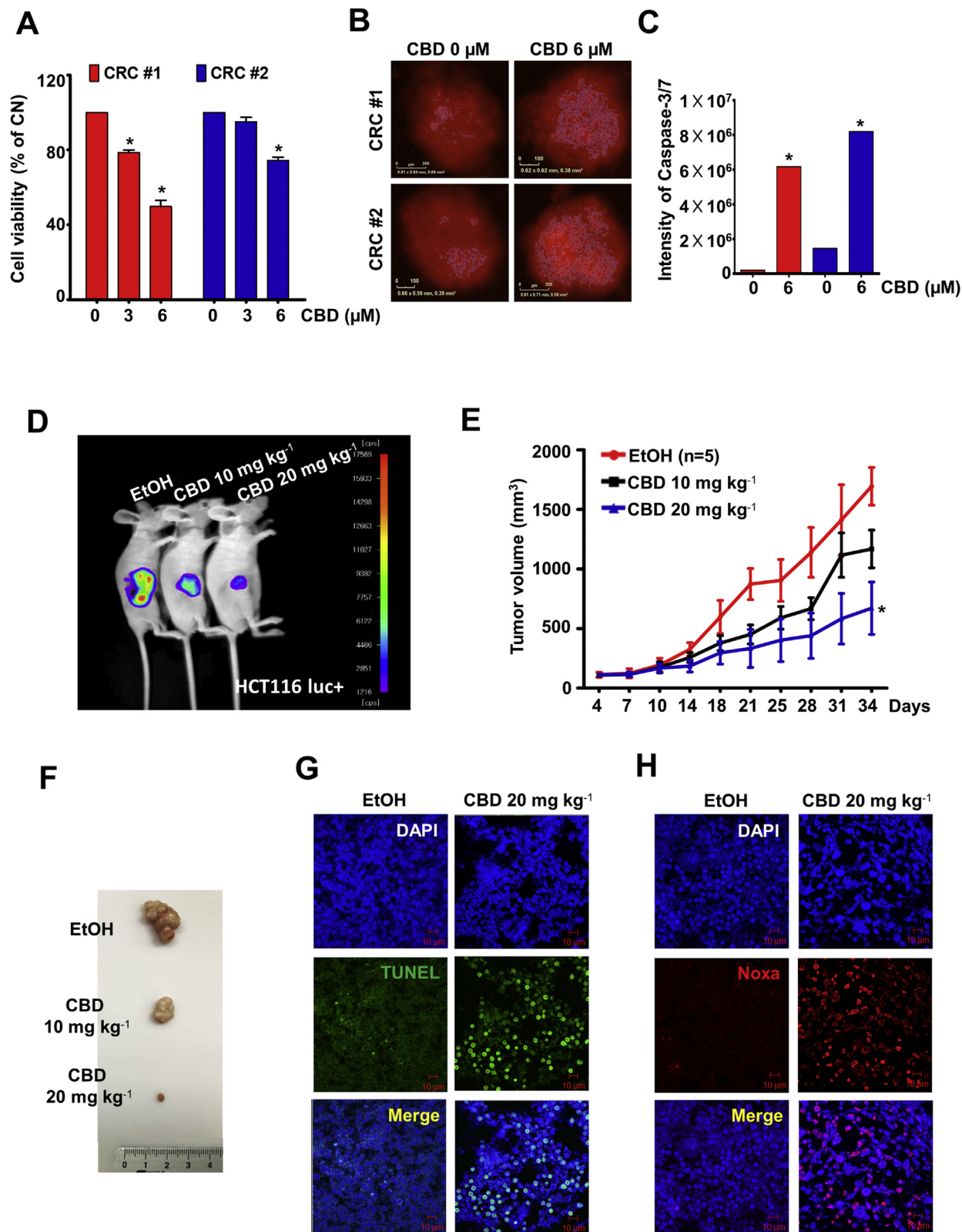


Fig. 5. CBD upregulates Noxa and CHOP expression, and it leads to *in vivo* apoptosis. (A) The cell viability was detected in two PDC cells by WST-1 assay. (B–C) The Caspase 3/7 dye was added to the media after the CBD treatment, and incubated in IncuCyte ZOOM for 3 days. The intensity of Caspase 3/7 fluorescence was then analyzed by IncuCyte Live-Cell Analysis system (B) and the graph was represented by Image J (C). (D–H) HCT116 Luc⁺ cells (1×10^7) were subcutaneously injected into BALB/c nude mice and were raised until the tumor size reached 150 mm³. Five mice were analyzed in each group. (D) The mice were captured by Image J. (E) The EtOH or CBD (10 mg/kg or 20 mg/kg) was intraperitoneally treated to the mice and the tumor size was measured once in three days and (F) the photographs of tumor were taken using a digital camera. (G) Apoptosis in tissue was detected by TUNEL assay (light green) and (H) Noxa expression (red) has increased after CBD treatment (20 mg/kg). The data were observed by confocal microscopy and nuclei were co-stained with DAPI solution (Scale Bar, 10 μm). (For interpretation of the references to color in this figure legend, the reader is referred to the Web version of this article.)

In addition to confirm that ER stress was regulated by ROS, the cells were treated with the ROS scavenger NAC along with CBD. As shown in Fig. 4E, CBD remarkably increased ER stress-related proteins, and NAC partially reversed this effect of CBD, suggesting that ROS induced by CBD contributes to the increased expression levels of Noxa via ER stress.

3.5. CBD inhibits tumor growth *in vivo* by upregulating the expression of noxa, thereby inducing apoptosis

To verify the results obtained, we used two PDC cell lines. As shown as Fig. 5A, CBD diminished the viability of PDC cell lines. In addition, the intensity of Caspase 3/7-stained cells was increased by CBD treatment in PDC cell spheroids in three-dimensional culture (Fig. 5B and C).

Next, we examined the effect of CBD on the tumorigenicity ability *in vivo*. The HCT116 Luc⁺ cells (1×10^7 in 100 μ L) were subcutaneously injected into BALB/c nude mice, and the tumor size was measured twice a week. When the tumor size was 150 mm³, the luminescence and tumor size in CBD-treated mice were markedly lower than those in the control mice (Fig. 5D, E and 5F), suggesting that CBD decreases the growth of CRC cells *in vivo*. To unveil whether apoptosis plays a role in CBD-induced growth inhibition, we performed TUNEL assay and immunohistochemistry on the tumor tissue. The number of TUNEL-positive cells and the level of Noxa protein were higher in CBD-injected tumors, compared to the control tumors (Fig. 5G and H), indicating that CBD induces apoptosis *in vivo* by Noxa activation.

4. Discussion

Because of the different problems associated with the chemotherapeutic drugs currently used for CRC, many studies have concentrated on alternative therapies that are safer and less toxic such as those employing natural products [20]. In this study, we focused on the cytotoxic effect exerted by the natural product CBD. Previous studies have suggested that the anticancer effect of CBD is associated with its ability to induce apoptosis; in fact, several related signaling pathways have been reported [14,19,25,27]. We explored the mechanisms by which CBD mediated apoptosis in human CRC cell lines and investigated the complex relationship between CBD-induced Noxa activation, apoptosis, and generation of ROS/ER stress.

We found that CBD induced dose-dependent growth inhibition and apoptosis in human CRC cells, but not in normal colorectal cells. Apoptosis induction was confirmed by the cleavage of PARP and caspase-3, caspase-8, and caspase-9. Moreover, CBD increased the number of Annexin V/PI double-positive cells and TUNEL-positive cells. CBD also decreased tumor volume and promoted apoptosis in a xenograft model. In the xenograft model using prostate cancer cells, an adverse effect was not observed when 100 mg/kg CBD was injected daily for 5 weeks. Thus, the 20 mg/kg dose used in our experiment did not exert any adverse effect on the mice [7].

One major finding of this study is that Noxa activation is important for CBD-induced apoptosis in human CRC cells; this has not been reported previously, to the best of our knowledge. The expression of Bcl-2 Homology 3 domain-only protein, namely, Noxa, was increased by CBD treatment in a dose- and time-dependent manner. Unfortunately, CBD did not affect other Bcl-2 family member proteins except truncated BID (t-BID), which was activated later timepoint than when Noxa was activated (data not shown). After CBD treatment, MMP was decreased and ROS was produced in a noticeably short time, suggesting that when CBD-induced apoptosis occurs, CBD induces mitochondrial dysfunction directly rather than through other Bcl-2 family proteins. In addition, CBD induced Noxa activation and apoptosis, which could be blocked by siRNA knockdown of Noxa. Noxa expression is regulated by p53 [18]. However, in our system, CBD treatment did not cause any changes in the Noxa levels and cell death in the p53 knockout CRC cell lines, implying that CBD causes Noxa-induced apoptosis through the p53-independent pathway.

Excessive ROS is considered to be toxic, with the ability to induce oxidative damage to biological macromolecules, initiating the peroxidation of membrane lipids and causing the accumulation of lipid peroxides and damage of DNA and proteins [30]. Mitochondria are the major cellular organelles producing ROS, and within the mitochondrion, the electron transport chain is the primary site of ROS generation [36]. CBD elevated the oxygen consumption rate and enhanced mitochondrial bioenergetics by regulating the mitochondrial complex I and IV [28]. From this point of view, it seems that the CBD-induced mitochondrial ROS overproduction in CRC cells was caused by the regulatory effects of CBD on mitochondrial complex I and IV. However, further studies are necessary to unveil the mechanisms responsible for excessive mitochondrial ROS generation by CBD-treated CRC cells. Moreover, Noxa caused ROS production, which is likely to further exacerbate the apoptosis induced by CBD [10]. Thus, these findings together suggest that CBD induces apoptosis of CRC cells by triggering mitochondrial dysfunction.

ROS is well-known ER stress inducer [35]. ER stress triggers the activation of UPR, which functions as an adaptive response and further leads to apoptosis [35]. UPR is distinguished by three ER transmembrane receptor proteins, namely, IRE1 α , PERK, and ATF6 [21]. In resting cells, all three receptors are associated with the ER resident chaperone Bip, which maintains them in an inactive state. On accumulation of unfolded proteins in the ER, the three receptors dissociate from Bip, leading to their activation. On activation, the three receptors induce signal transduction, which reduces the accumulation of misfolded proteins by increasing the expression of ER chaperones [21,29]. Consistent with this, we found that the expression of ER stress-related genes was reduced in CBD-treated CRC cells, and that it is regulated by ROS. NAC, a ROS scavenger, effectively blocked CBD-induced generation of ROS and ER stress and attenuated CBD-induced apoptotic cell death. Moreover, ROS and ER stress are associated with Noxa activation. Interestingly, CHOP indirectly regulates Noxa activation. We speculated that activating transcription factor 3 (ATF3) and ATF4 are involved in CBD-induced CHOP and Noxa activation. ER stress activates ATF3 and ATF4 and increases their complex formation to activate Noxa and CHOP [15]. Our results showed that ATF3 and ATF4 bind directly to ATF/cAMP responsive element-binding sites in the promoter regions of Noxa and CHOP, inducing CBD-induced Noxa and CHOP activation. Thus, CBD-induced Noxa and CHOP are expected to be mediated by upregulation of ATF3 and ATF4 binding to their promoter regions.

To summarize, CBD induces apoptotic cell death in CRC cells. This increase in apoptosis can be attributed to its ability to trigger the generation of excessive mitochondrial ROS and ER stress and subsequent activation of Noxa (Fig. 6). Thus, our results provide important evidence for the use of CBD as an alternative therapeutic agent for CRC.

Conflicts of interest

No potential conflicts of interest to declare.

Authors' contributions

Soyeon Jeong and Hye Kyeong Yun participated in study design and conception, execution of the experiments, data analysis and interpretation, and manuscript writing; Yoon A Jeong participated in mice tumor tissue processing and immunofluorescence of tumor tissue; Min Jee Jo participated in the primary culture of patient derived CRC cells and *in vivo* experiments; Sang Hee Kang participated in the study conception and analysis of microarray data; Jung Lim Kim and Dae Yeong Kim participated in the collection and assembly of data and *in vivo* experiments; Sun Il Lee, Seong Hae Park, Bo Ram Kim and Yoo Jin Na participated in interpretation of data and designing of figures; Han Do Kim and Dae Hyun Kim provided Cannabidiol; Dae-Hee Lee and Sang Cheul Oh participated in the conception and design, financial support, interpretation of study, and supervised all of the experiments. All

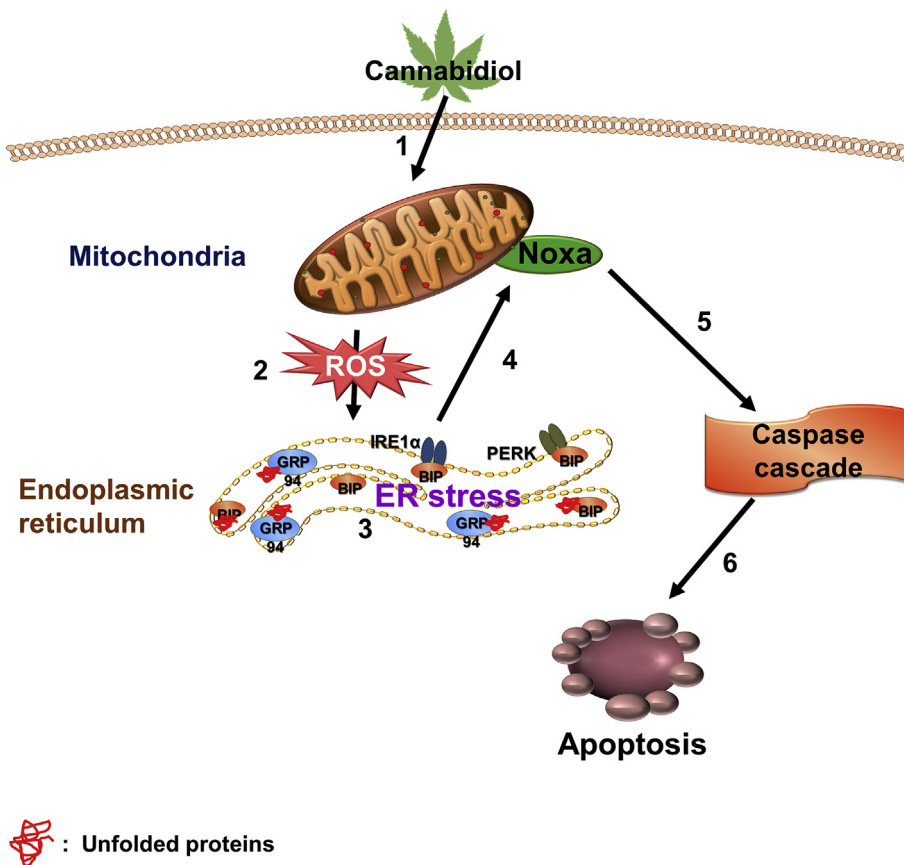


Fig. 6. Scheme of apoptosis pathway induced by CBD.

authors approved the submission of the final manuscript.

Acknowledgements

This work was supported by the National Research Foundation of Korea grant funded by the Korea government (MSIP) (NRF-2017R1D1A1B03030703) and supported by the Business for Cooperative R & D between Industry, Academy, and Research Institute funded Korea Small and Medium Business Administration in 20 (C0566291) and a Korea University Grant.

Appendix A. Supplementary data

Supplementary data to this article can be found online at <https://doi.org/10.1016/j.canlet.2019.01.011>.

References

- [1] A. Banerjee, V. Banerjee, S. Czinn, T. Blanchard, Increased reactive oxygen species levels cause ER stress and cytotoxicity in andrographolide treated colon cancer cells, *Oncotarget* 8 (2017) 26142–26153.
- [2] B. Chakravarti, J. Ravi, R.K. Ganju, Cannabinoids as therapeutic agents in cancer: current status and future implications, *Oncotarget* 5 (2014) 5852–5872.
- [3] B. D'Autreaux, M.B. Toledano, ROS as signalling molecules: mechanisms that generate specificity in ROS homeostasis, *Nat. Rev. Mol. Cell Biol.* 8 (2007) 813–824.
- [4] H. Ehrhardt, I. Hofig, F. Wachter, P. Obexer, S. Fulda, N. Terziyska, I. Jeremias, NOXA as critical mediator for drug combinations in polychemotherapy, *Cell Death Dis.* 3 (2012) e327.
- [5] M. Guzman, Cannabinoids: potential anticancer agents, *Nat. Rev. Canc.* 3 (2003) 745–755.
- [6] N. Hatsugai, V. Perez Koldenkova, H. Imamura, H. Noji, T. Nagai, Changes in cytosolic ATP levels and intracellular morphology during bacteria-induced hypersensitive cell death as revealed by real-time fluorescence microscopy imaging, *Plant Cell Physiol.* 53 (2012) 1768–1775.
- [7] K. Iffland, F. Grotenhermen, An update on safety and side effects of cannabidiol: a review of clinical data and relevant animal studies, *Cannabis Cannabinoid Res.* 2 (2017) 139–154.
- [8] S. Jeong, K. Jing, N. Kim, S. Shin, S. Kim, K.S. Song, J.Y. Heo, J.H. Park, K.S. Seo, J. Han, T. Wu, G.R. Kweon, S.K. Park, J.I. Park, K. Lim, Docosahexaenoic acid-induced apoptosis is mediated by activation of mitogen-activated protein kinases in human cancer cells, *BMC Canc.* 14 (2014) 481.
- [9] K. Jing, K.S. Song, S. Shin, N. Kim, S. Jeong, H.R. Oh, J.H. Park, K.S. Seo, J.Y. Heo, J. Han, J.I. Park, C. Han, T. Wu, G.R. Kweon, S.K. Park, W.H. Yoon, B.D. Hwang, K. Lim, Docosahexaenoic acid induces autophagy through p53/AMPK/mTOR signaling and promotes apoptosis in human cancer cells harboring wild-type p53, *Autophagy* 7 (2011) 1348–1358.
- [10] J.Y. Kim, H.J. Ahn, J.H. Ryu, K. Suk, J.H. Park, BH3-only protein Noxa is a mediator of hypoxic cell death induced by hypoxia-inducible factor 1alpha, *J. Exp. Med.* 199 (2004) 113–124.
- [11] V. Labi, M. Erlacher, S. Kiessling, A. Villunger, BH3-only proteins in cell death initiation, malignant disease and anticancer therapy, *Cell Death Differ.* 13 (2006) 1325–1338.
- [12] G. Lenaz, The mitochondrial production of reactive oxygen species: mechanisms and implications in human pathology, *IUBMB Life* 52 (2001) 159–164.
- [13] J.D. Malhotra, R.J. Kaufman, Endoplasmic reticulum stress and oxidative stress: a vicious cycle or a double-edged sword? *Antioxidants Redox Signal.* 9 (2007) 2277–2293.
- [14] M. Nabissi, M.B. Morelli, M. Santoni, G. Santoni, Triggering of the TRPV2 channel by cannabidiol sensitizes glioblastoma cells to cytotoxic chemotherapeutic agents, *Carcinogenesis* 34 (2013) 48–57.
- [15] T. Narita, M. Ri, A. Masaki, F. Mori, A. Ito, S. Kusumoto, T. Ishida, H. Komatsu, S. Iida, Lower expression of activating transcription factors 3 and 4 correlates with shorter progression-free survival in multiple myeloma patients receiving bortezomib plus dexamethasone therapy, *Blood cancer J* 5 (2015) e373.
- [16] E. Oda, R. Ohki, H. Murasawa, J. Nemoto, T. Shibue, T. Yamashita, T. Tokino, T. Taniguchi, N. Tanaka, Noxa, a BH3-only member of the Bcl-2 family and candidate mediator of p53-induced apoptosis, *Science* 288 (2000) 1053–1058.
- [17] M.S. Ola, M. Nawaz, H. Ahsan, Role of Bcl-2 family proteins and caspases in the regulation of apoptosis, *Mol. Cell. Biochem.* 351 (2011) 41–58.
- [18] C. Ploner, R. Kofler, A. Villunger, Noxa: at the tip of the balance between life and death, *Oncogene* 27 (Suppl 1) (2008) S84–S92.
- [19] R. Ramer, K. Heinemann, J. Merkord, H. Rohde, A. Salamon, M. Linnebacher, B. Hinz, COX-2 and PPAR-gamma confer cannabidiol-induced apoptosis of human lung cancer cells, *Mol. Canc. Therapeut.* 12 (2013) 69–82.
- [20] S.K. Saha, A.R. Khuda-Bukhs, Molecular approaches towards development of purified natural products and their structurally known derivatives as efficient anti-cancer drugs: current trends, *Eur. J. Clin. Pharmacol.* 714 (2013) 239–248.
- [21] R. Sano, J.C. Reed, ER stress-induced cell death mechanisms, *Biochim. Biophys.*

- Acta 1833 (2013) 3460–3470.
- [22] Y.W. Seo, J.N. Shin, K.H. Ko, J.H. Cha, J.Y. Park, B.R. Lee, C.W. Yun, Y.M. Kim, D.W. Seol, D.W. Kim, X.M. Yin, T.H. Kim, The molecular mechanism of Noxa-induced mitochondrial dysfunction in p53-mediated cell death, *J. Biol. Chem.* 278 (2003) 48292–48299.
- [23] T. Shibue, S. Suzuki, H. Okamoto, H. Yoshida, Y. Ohba, A. Takaoka, T. Taniguchi, Differential contribution of Puma and Noxa in dual regulation of p53-mediated apoptotic pathways, *EMBO J.* 25 (2006) 4952–4962.
- [24] T. Shibue, K. Takeda, E. Oda, H. Tanaka, H. Murasawa, A. Takaoka, Y. Morishita, S. Akira, T. Taniguchi, N. Tanaka, Integral role of Noxa in p53-mediated apoptotic response, *Genes Dev.* 17 (2003) 2233–2238.
- [25] A. Shrivastava, P.M. Kuzontkoski, J.E. Groopman, A. Prasad, Cannabidiol induces programmed cell death in breast cancer cells by coordinating the cross-talk between apoptosis and autophagy, *Mol. Canc. Therapeut.* 10 (2011) 1161–1172.
- [26] R.L. Siegel, K.D. Miller, A. Jemal, Cancer statistics, 2017, *CA A Cancer J. Clin.* 67 (2017) 7–30.
- [27] S. Sreevalsan, S. Joseph, I. Jutooru, G. Chadalapaka, S.H. Safe, Induction of apoptosis by cannabinoids in prostate and colon cancer cells is phosphatase dependent, *Anticancer Res.* 31 (2011) 3799–3807.
- [28] S. Sun, F. Hu, J. Wu, S. Zhang, Cannabidiol attenuates OGD/R-induced damage by enhancing mitochondrial bioenergetics and modulating glucose metabolism via pentose-phosphate pathway in hippocampal neurons, *Redox Biol.* 11 (2017) 577–585.
- [29] E. Szegezdi, S.E. Logue, A.M. Gorman, A. Samali, Mediators of endoplasmic reticulum stress-induced apoptosis, *EMBO Rep.* 7 (2006) 880–885.
- [30] B. Uttara, A.V. Singh, P. Zamboni, R.T. Mahajan, Oxidative stress and neurodegenerative diseases: a review of upstream and downstream antioxidant therapeutic options, *Curr. Neuropharmacol.* 7 (2009) 65–74.
- [31] G. Velasco, S. Hernandez-Tiedra, D. Davila, M. Lorente, The use of cannabinoids as anticancer agents, *Prog. Neuro-Psychopharmacol. Biol. Psychiatry* 64 (2016) 259–266.
- [32] G. Velasco, C. Sanchez, M. Guzman, Towards the use of cannabinoids as antitumour agents, *Nat. Rev. Canc.* 12 (2012) 436–444.
- [33] G. Velasco, C. Sanchez, M. Guzman, Anticancer mechanisms of cannabinoids, *Curr. Oncol.* 23 (2016) S23–S32.
- [34] Y. Yang, Y. Zhang, L. Wang, S. Lee, Levistolid A induces apoptosis via ROS-mediated ER stress pathway in colon cancer cells, *Cell. Physiol. Biochem.* 42 (2017) 929–938.
- [35] Y. Yuan, X. Xu, C. Zhao, M. Zhao, H. Wang, B. Zhang, N. Wang, H. Mao, A. Zhang, C. Xing, The roles of oxidative stress, endoplasmic reticulum stress, and autophagy in aldosterone/mineralocorticoid receptor-induced podocyte injury, *Lab. Invest.* 95 (2015) 1374–1386.
- [36] D.X. Zhang, D.D. Gutterman, Mitochondrial reactive oxygen species-mediated signaling in endothelial cells, *Am. J. Physiol. Heart Circ. Physiol.* 292 (2007) H2023–H2031.
- [37] D.B. Zorov, M. Juhaszova, S.J. Sollott, Mitochondrial reactive oxygen species (ROS) and ROS-induced ROS release, *Physiol. Rev.* 94 (2014) 909–950.